DOI: 10.1002/
Article type: Full Paper

Theoretical investigation of phase transitions of graphite and cubic 3C diamond into hexagonal 2H diamond under high pressures

Vladimir A. Greshnyakov, Evgeny A. Belenkov, Maria M. Brzhezinskaya*

Dr. V. A. Greshnyakov, Prof. E. A. Belenkov
Chelyabinsk State University, Bratiev Kashirinih 129, 454001 Chelyabinsk, Russia
E-mail: belenkov@csu.ru
Dr. M. M. Brzhezinskaya
Helmholtz-Zentrum Berlin für Materialien und Energie, Institute for Nanometer Optics and Technology, Albert-Einstein-Strasse 15, 12489 Berlin, Germany

Keywords: diamond, polytypes, graphite, high pressure synthesis, simulation

Possible techniques for experimentally obtaining hexagonal diamond were studied in the scope of the density functional theory method. It has been found out that hexagonal diamond may be created as a result of structural transition at the 61 to 68 GPa uniaxial compression from orthorhombic AB graphite and at 57 to 66 GPa from hexagonal AA graphite. Also formation of hexagonal diamond was shown to take place in case of very strong (300 to 380 GPa) compression of cubic diamond. X-ray and electron-microscopic data on nanodiamonds from meteorite craters were analyzed for the presence of hexagonal diamond. The analysis has shown that impact-origin carbon materials do not contain pure cubic and hexagonal diamonds, and layers of nascent crystals of diamond polytypes are randomly packed.

1. Introduction

Among all the known materials, cubic diamond is characterized by extremely high mechanical strength.[1–3] However, paper[4] reported that hexagonal 2*H* diamond may be even stronger. Since diamond films are widely used as coatings of cutting tools and machine components in order to improve their corrosion and wear resistance,[5,6] studying of this issue

is indeed of great practical interest. The increase in the diamond film strength due to formation of the 2*H* diamond polytype structure can considerably improve the quality of diamond films used in the mentioned field. However, it is quite difficult to experimentally verify this theoretical estimate of strength because all attempts to obtain pure 2*H* diamond polytype has failed up to now. Some researchers report that hexagonal diamonds have been found in meteorite crater rocks[7,8] and also from meteorite residues.[9] Carbon phases of these rocks called «lonsdaleite» exhibit the presence of 2*H* diamond polytype.[7] Yet the studies carried out in recent years showed that the mineral called «lonsdaleite» is not pure 2*H* diamond polytype.[10] At best, the carbon component of this mineral is a mixture of 2*H* and 3C polytypes[11] or diamond-like material with randomly packed layers.[10,12] Various methods for synthesizing artificial diamonds almost always produce only cubic diamond.[1,2,13–15] To reliably confirm that hardness of 2*H* diamond polytype is higher than that of 3*C* diamond polytype, it is necessary to synthesize 2*H* polytype. For this purpose, conditions under which formation of hexagonal diamond is possible should be analyzed. Therefore, in this study theoretical calculations were performed for phase transitions of various structural modifications of graphite to cubic and hexagonal diamonds and of cubic diamond to hexagonal diamond.

Another important aspect to be considered concerns the analysis of experimental techniques that could unambiguously identify the diamond polytypes. All the previously reported experimental results based on which the conclusion on the existence of hexagonal diamond polytype has been made are ambiguous[10] and differently interpretable.[11,12] Hence, establishing of rigorous criteria for the 2*H* diamond polytype identification appeared to be necessary, which has been just accomplished in this work.

2. Calculation Techniques

A priory, the phase transitions were assumed to occur due to deformation of crystal lattices.[10,14–17] As one of the main methods to experimentally obtain diamond-like phases is exposure of graphite-like materials to high pressure,[1,13] possible precursors of hexagonal diamond consisting of sp^2-hybridized carbon atoms were theoretically analyzed. The theoretical analysis showed that *Cmmm* and *P*6/*mmm* graphites with the AB and AA graphene layers packing, respectively, may be used as the sp^2-precursors. According to calculations performed in [18], the *Cmmm* graphite is metastable and, hence, it may be used as an initial phase, while the *P*6/*mmm* graphite is unstable and transforms into the 2*H* or 3*R* modification. However, the *P*6/*mmm* graphite structure can be obtained by applying stresses of two types that stimulate compression of the initial graphite structure along the [001] axis and shear strain of the graphene layers along the [100] axis. In addition, hexagonal diamond can be obtained from cubic diamond.

Unit cells of the AB and AA graphites and cubic and hexagonal diamonds were chosen so that the numbers of their atoms were identical and equal to sixteen (Figure 1). The AB *Cmmm* graphite (Figure 1d) differed from the AA *P*6/*mmm* graphite (Figure 1e) in the order of graphene layers packing. For the cubic diamond, two different unit cells were chosen (Figures 1b and 1c) in order to ensure their matching with those of the AB and AA graphites. In the process of the phase transition, the atom positions, elementary translation vector lengths and crystal lattice type change so that the initial phase structure transforms into the final phase structure. Structural transformations of such a type are possible only in case of a certain mutual orientation of the phase crystal lattices. For the «AB graphite → cubic diamond» and «AB graphite → hexagonal diamond» phase transitions, strain directions were chosen as follows: [001] for graphite, [211] for cubic diamond, and [100] for hexagonal diamond. In the case of phase transitions «AA graphite → cubic diamond» and «AA graphite → hexagonal diamond», the [001] strain direction was chosen for graphite, [110] for cubic diamond, [001]

and [110] for hexagonal diamond. The «graphites → cubic diamond» phase transitions were considered in order to find the conditions when formation of hexagonal diamond from graphite is more favorable than of cubic diamond. In simulating the «cubic diamond → hexagonal diamond» phase transition, three types of the crystal lattice orientations for 3*C* and 2*H* diamonds were considered, namely, [110]-[001], [110]-[110] and [211]-[100].

The modeling of phase transitions consisted in calculating the total energy of the structures in their initial and final states and also energies of structures uniaxially strained in the above directions. The structure strains were defined by stepwise incrementing of elementary translation vector lengths and respective variations in relative coordinates of the unit cell atoms. Pressures corresponding to different deformation extents were calculated as the total energy second derivative with respect to volume.

The calculations were performed using the Quantum ESPRESSO code[19] by the density functional theory (DFT) method.[20] In calculation, the Perdew-Zunger exchange-correlation energy functionals[21] were used in the local density approximation (LDA) and Perdew-Burke-Ernzerhof functionals[22] in the general gradient approximation (GGA). Only valence electrons were considered in calculation. The ion core effect was considered through the norm-conserving Troullier-Martins pseudopotential.[23] In integrating over the Brillouin zones, *k*-point 12×12×12 grids chosen according to the Monkhorst-Pack sampling scheme[24] were used. Wave functions were expanded with respect to a truncated basis set of plane waves. The kinetic energy cut-off was set to 60 Ry. Geometric optimization of the structures under consideration was continued until the forces and stresses become lower than 1 meV/Å and 0.5 GPa, respectively.

The technique of DFT calculation of carbon compounds was approbated by comparing the calculated and measured unit cell parameters of cubic diamond ($Fd\bar{3}m$) and hexagonal graphite ($P6_3/mmc$). Calculated covalent bond lengths in diamond and graphite differ from the respective experimental values [1] by ≤ 3.5%. Differences between the experimental[1] and

theoretical values of the graphite interlayer distances are 4.5% for the DFT-LDA method and 10.5 % for DFT-GGA.

The possibility of unambiguous identification of a diamond polytype was analyzed in the process of theoretically simulating X-ray powder patterns of carbon structures. The X-ray patterns were calculated by the standard method.[25] The diffraction maxima profiles were approximated by the pseudo-Voigt functions and calculated for the cases of CuK_α and MoK_α radiation.

3. Results of simulating phase transitions of graphites to hexagonal and cubic diamonds

At the first stage of investigation, geometrically optimized unit cells of hexagonal diamond (Figure 1a), cubic diamond (Figures 1b and 1c), orthorhombic and hexagonal graphites (Figures 1d and 1e, respectively) were calculated. Table 1 presents the unit cell parameters, equilibrium atomic volumes (V_0) and total energies for carbon structures free of external stresses. The minimal total energy is observed for cubic diamond in case of DFT-LDA calculations and for the AB graphite in case of DFT-GGA calculations. Total energies of thee phases differ insignificantly (by ~ 0.1 eV/atom).

At the second stage of calculations, the initial crystal structures of graphites were smoothly compressed along the axes perpendicular to the graphene layer planes. Crystallographic strain directions are shown in Table 2. The strain is continued until all the atoms transfer from the three-coordinated (sp^2) state to the four-coordinated (sp^3) state.

Figure 2 represents the dependences of total energy (E_{total}) on atomic volume (V_{at}) for orthorhombic AB graphite as well as for cubic (3*C*) and hexagonal (2*H*) diamonds, which characterize direct and reverse transitions between these phases. The phase atomic volumes changed due to crystal lattices strains caused by the stresses generated by external pressures (Figure 3). Structural transformation of the AB graphite to hexagonal diamond results from overcoming the 0.241 to 0.337 eV/atom energy barrier (Figure 2, Table 2) at the atomic

volume of ~ 6.4 Å^3/atom when the pressure reaches 61-68 GPa (Figure 3). Such thermodynamic parameters initiate the graphite to cubic diamond phase transition. The «AB graphite → hexagonal diamond» structural transition is the first-order transition at which the atomic volume changes stepwise by 14 % (Figure 3). The design difference in enthalpies of the initial and final phases in formation of hexagonal diamond is ΔH = -0.67 (-0.58) eV/atom, which indicates the exothermic character of the structural transformation.

Plots illustrating the AA graphite to hexagonal and cubic diamonds phase transitions are given in Figure 4. Hexagonal diamond may be obtained by increasing the graphite atomic volume to 6.453 (6.599) Å^3/atom that corresponds to the pressure of 57-68 GPa (Table 2). In the course of this phase transition, the volume decreases by 15-16 %, and energy of 0.65-0.81 eV/atom may be released. As the pressure of the AA graphite structural transition to hexagonal diamond is lower than design values of corresponding pressures of phase transitions to cubic diamond (Table 2) and diamond-like phases LA3 (bct C_4), LA5 (Y-carbon), LA6 and LA7,[10] its formation from the *P*6/*mmm* graphite should occur earlier than formation of other diamond-like structures.

In addition, energy barriers ($\Delta E_{D\text{-}G}$) for transitions of diamond-like structures (*D*) to graphite (*G*) structures were determined. These barriers characterize the stability of one or another compound consisting of four-coordinated atoms to pressure and temperature variations. The reverse transition of hexagonal diamond to AB graphite needs overcoming the energy barrier of 0.310 (0.246) eV/atom for extension of its structure along [100] (Figure 2). Hexagonal diamond may be transformed into the AA graphite by extending its structure along crystallographic directions [001] and [110]. In these cases, $\Delta E_{D\text{-}G}$ values are 0.361 (0.303) and 0.383 (0.317) eV/atom, respectively (Figure 4). The minimal $\Delta E_{D\text{-}G}$ of hexagonal diamond essentially exceeds the respective barriers of the LA3 and LA5 diamond-like phases,[10] which indicates its high thermal stability as compared with other diamond-like phases with equivalent atom positions.[13] The minimal energy barrier for the hexagonal diamond to

graphite transition is only 1 to 2% lower than that for cubic diamond.[10] Hence, the phase transition temperature should be lower than that of the «cubic diamond [111] → graphite ABC [001]» transition by the same value.

Thus, hexagonal diamond may be obtained from the AA graphite by uniaxial compression in the [001] direction. At this compression only the 2*H* polytype of diamond should arise. Uniaxial compression of the AB graphite along the [001] axis can cause formation of both the 2*H* and 3*C* polytypes. Thus only the first synthesis technique should be chosen for obtaining pure 2*H* polytype.

4. Results of simulating the cubic diamond to hexagonal diamond phase transition

Hexagonal diamond may be obtained by the uniaxial static compression of cubic diamond along the crystallographic [110]-axis (Table 2). Figure 5 represents the calculations of total energy and volume per atom for the cases of compression and decompression of the diamond-like phases. The hexagonal diamond strained in the [110] direction was shown to be creatable from cubic diamond at the volume V_{at} decrease to 4.745 (4.983) Å^3/atom (Figure 5) corresponding to the pressure of 380 (300) GPa.

Another way of obtaining the 2*H* diamond is uniaxial compression of cubic diamond along the [211]-axis (Table 2, Figure 6). In this case, the 2*H* diamond polytype is created which is deformed along the [100]-axis at V_{trans} ~ 5.0 Å^3/atom corresponding to the pressure of 303 (354) GPa.

Thus, hexagonal diamond may be obtained by compressing cubic diamond. Pressures necessary to form hexagonal diamond by compressing the 3*C* diamond along the [110]- and [211]-axes may be assumed to be approximately equal to each other and range from 300 to 380 GPa. These results agree well with experimental data from paper [26] devoted to studying pulsed laser irradiation of pyrolytic graphite resulting first in the graphite transformation into

the 3*C* diamond at 60 GPa and then, at the pressure of ~ 215 GPa, in the 3*C* diamond transformation into the 2*H* diamond polytype.

5. Possibility analysis of experimental diffraction identification of diamond polytypes

Cubic diamond, diamond polytypes and various diamond-like materials occur in different minerals[5–8,27–29] and also may be obtained artificially by different methods.[1,2,13,30–35] Previous paragraphs present the calculations confirming theoretical possibility of the 2*H* polytype synthesis. The question now arises of what will be a conclusive proof of the fact that just this polytype has been obtained in experiments but not synthesized earlier in any other way. The best methods for identifying the diamond polytype in these materials are such diffraction methods as X-ray structure analysis and electron diffraction. However, a number of authors are in doubt upon the reliability of the 2*H* diamond polytype identification in various diamond-like materials.[8-10] Below we present analysis of data confirming that hexagonal diamond has been experimentally observed.

The hexagonal diamond synthesis was reported for the first time in the paper by Bundy and Casper.[30] In this study they obtained a Debye powder pattern of a polycrystal diamond material exhibiting a set of diffraction rings characteristic of the 2*H* diamond polytype. Based on these data, a conclusion was made that «pure» hexagonal diamond was synthesized. Nevertheless, these data may be interpreted in another way. Let the diamond structure have random layer packing, which means that hexagonal layers randomly alternate with non-hexagonal layers. We have theoretically simulated X-ray patterns for this case.

For this purpose, we considered crystals with the diamond-like structure and hexagonal or trigonal unit cells containing up to sixty diamond layers along the *c*-axis. Then we set different probabilities (P_h) of the hexagonal layer occurrence in the unit cell. The considered probabilities P_h ranged from 0 to 100 %. X-ray patterns corresponding to the chosen probabilities were created by combining individual X-ray patterns obtained for crystals in

which hexagonal layers could be observed with probability P_h. Unit cells of such crystals were generated randomly. The number of such crystals used to construct a certain integrated X-ray pattern was 10^6. Broadening of X-ray patterns peaks was simulated assuming that the average crystal size was 150 Å. In the case of P_h = 100 %, the obtained X-ray pattern of polycrystalline hexagonal diamond was of the conventional type (Figure 7a).[10,30,36] When P_h decreased to 75 %, diffraction peaks 101, 102 and 103 became considerably broader and, at the same time, less intense. Thus, it is possible to observe all the diffraction peaks characteristic of hexagonal diamond (Figure 7a) more than 3.5 % in intensity in diamond-like crystals whose structure differs markedly from 2*H* polytype. Such crystals contain a large number of packing defects, so that their mean hexagonality is 78 % at P_h ~ 80 %, while hexagonality of the 2*H* polytype should be 100 %. Hence, authors of [30] might obtain not pure 2*H* diamond polytype but a highly hexagonal diamond-like material with a large number of packing defects.

There are also reports on revealing hexagonal diamond in the detonation synthesis products or carbon-containing minerals found at the places of meteorite impact.[33] X-ray patterns of such diamond-like materials exhibit typically three basic diffraction maxima related to d_{002}, d_{110} and d_{112} for hexagonal diamond. At the same time, the X-ray patterns do not contain maximum 102, while the position of strongly smeared maximum 103 is hardly definable. These diffraction patterns are conventionally interpreted as X-ray patterns of a mixture of two diamond polytypes (3*C* and 2*H*). However, in this case maxima 102 and 103 must be observed because the resulting X-ray pattern should be a superposition of the 2*H* and 3*C* polytype patterns. The absence of these maxima may be explained by disordered layer packing.[8] Let us justify this assumption by calculating relevant theoretical X-ray patterns. For this purpose, let us consider diamond polytypes mixtures with randomly packed layers (P_h = 50 %). Since detonation diamonds are nanosized, the X-ray patterns were calculated for different mean crystal sizes (50 to 150 Å). Figure 8 presents case X-ray patterns at different

crystal sizes. Similarly to the experimental X-ray patterns,[8,33] these model patterns do not exhibit hexagonal diamond maxima 102 and 103. In addition, one can see that the crystallite size reduction to 65 Å makes several main maxima merge into an asymmetric maximum whose shape perfectly fits those of experimentally observed diffraction maxima.[8,33] Hence, one can be sure that diamond-like materials arising in impact actions consist of nanocrystals with randomly packed layers.

Since hexagonal diamond is observed in nanocrystalline diamond-like materials, the 2*H* polytype identification is often performed by using electron microscopy enabling investigation of the structure in local microvolumes of the material.[8,27,32,35,37] As a rule, electron diffraction patterns of the diamond monocrystals or polycrystals demonstrated the 100, 002 and 101 maxima corresponding to the 2*H* diamond. However, identification of electron diffraction patterns may appear to be ambiguous.

Let us consider hexagonal polytypes consisting of *N* layers. One of the main conditions for observing a diffraction maximum is equality of the phase reciprocal lattice vector ($\vec{H}$) to the difference in wave vectors of scattered and projectile electrons. Elementary translation vectors $\vec{a}$ and $\vec{b}$ of lattices of various polytypes are equivalent, while the vector $\vec{c}$ length is equal to $d_{diam} \cdot N$, where d_{diam} is the interlayer distance corresponding to d_{111} of diamond. In this case, any reciprocal lattice vector may be defined as follows:

$$\vec{H} = h\vec{a}^{*} + k\vec{b}^{*} + 4\pi l\left[\vec{a} \times \vec{b}\right] / \left(\sqrt{3} N a^{2} d_{diam}\right),$$

where *h*, *k* and *l* are the Miller indices. This formula shows that different polytypes may have identical reciprocal lattice vectors, which makes ambiguous the results of diffraction patterns identification. For instance, maxima 100, 002 and 101 of the 2*H* polytype correspond to maxima 100, 004 and 102 of the 4*H* polytype, etc.

To say more, when the selected-area electron diffraction (SAED) method is used to study of nanodiamonds, electron diffraction patterns sometimes exhibit maximum 102

corresponding to the 2*H* diamond [8] which is not detected in X-ray patterns. The appearance of this diffraction maximum may be explained by that the electron beam scans a small nanodiamond part having packing defects, due to which the local area contains a large number of hexagonal layers, and its structure is close to that of the 2*H* polytype. When diffraction methods are used to study large material volumes, the results of diffraction from local areas with high and low hexagonality prove to be averaged. As a result, diffraction maximum 102 merges with the background, and the X-ray diffraction pattern becomes similar to that of the 3*C* polytype (Figure 8). Thus, the existence of the SAED reflex 102 cannot be a rigorous proof of the hexagonal diamond existence. Indeed, observation of the layer packing order in diamonds by high-resolution transmission electron microscopes[8,12,27,37] show that the 100 % hexagonality characteristic of the 2*H* polytype is not seen in nanodiamonds, which evidences the absence of pure 2*H* polytype.

6. Discussion

Comparative analysis of the experimental[5,8,30,31,35] and theoretical[9,10,36] results, as well as results of simulating diamond diffraction patterns we have presented (Figures 7 and 8), show that unambiguous identification of the 2*H* diamond by the diffraction methods is possible only if all the diffraction maxima characteristic of hexagonal diamond are reliably fixed. The exact correspondence should be for both the diffraction angles at which the maxima are observed, and the ratio of their intensities. Experimental studies reporting observation of the 2*H* polytype did not demonstrate exact fit. First of all it was caused by that structures of the majority of the studied diamond-like materials were of the nanocrystalline character, due to which the most intense 2*H* polytype diffraction maxima 100 ($d_{100} \approx 2.18$ Å), 002 ($d_{002} \approx 2.05$ Å) and 101 ($d_{101} \approx 1.93$ Å) merge into one broad asymmetric maximum because of significant smearing due to small crystal sizes. In the same diffraction angle range there should be highly intense maxima of other diamond and graphite polytypes. Therefore,

the diffraction maximum smearing may be interpreted from different points of view. The results of its decomposition based on the *a priory* assumption that it contains lines characteristic of the 2*H* polytype cannot be regarded as a rigorous prove of the hexagonal polytype existence. The presence of the 2*H* polytype could be reliably proved by the presence of maxima 102 ($d_{102} \approx 1.50$ Å) and 103 ($d_{103} \approx 1.17$ Å). However, as intensities of these peaks are low and comparable with that of the background radiation, they are hardly observable. These peaks were not revealed in most of papers that inform on observing the 2*H* polytype.[6,7,27,29,31,33–35] As one more indirect evidence of the polytype crystal structure perfection, transmission electron microscopy (TEM) observation of a defectless layered structure of diamond crystals may be regarded. However, most of TEM pictures of diamonds demonstrate disorder of layer packing. Thus, there are no reliable confirmations of experimental observation of pure 2*H* polytype. The reason for this may be that the ideal sequence of layer packing cannot be ensured in the process of the diamond structure formation. All diamond crystals contain someone or other number of hexagonal and non-hexagonal layers that may be regarded as packing defects from a certain point of view. For instance, any diamond crystal may be considered as a crystal having the 2*H* polytype structure containing a number of non-hexagonal layers regarded as packing defects. From another point of view, the same crystal may be considered as cubic (3*C*) diamond crystal whose hexagonal layers are packing defects. In reality, any diamond crystal seems to have random layer packing with different contents of hexagonal and non-hexagonal layers. To synthesize ideal polytypes from graphite, it is necessary that the initial graphite or diamond structure be also ideal. If layers of initial graphene have been randomly displaced from the ideal positions, then the formed diamond crystals have packing defects. The ideal packing of graphene layers in the initial graphite is nearly impossible since the layers are bound by weak van der Waals forces and can easily move relative to each other even at low stresses. Hence, diamonds, especially those synthesized by detonation techniques, should have randomly packed layers,

and the crystals cannot be classified as any polytype. Moreover, our calculations showed that pressures at which the 2*H* and 3*C* polytypes should be formed (*P* ~ 60 GPa), as well as sublimation energies of the polytypes, differ from each other only slightly (ΔE_{coh} ~ 0.03 eV/atom[38]). Therefore, different structural species of diamond can occur under the same conditions.

7. Conclusion

The studies performed, as well as analysis of experimental and theoretical works of other researchers, allowed us to ascertain that there are no reliable proofs of the 2*H* diamond polytype existence in minerals and artificially synthesized carbon materials. Theoretically, hexagonal diamond can be synthesized by compressing orthorhombic AB graphite. However, this needs the ideal graphene layer packing, which is almost impossible in the case of the detonation synthesis. If the graphene layer packing is disordered, diamond-like structures not fitting the ideal polytypes will be formed. In addition, formation of the 2*H* diamond is hindered since the AA graphite from which it can be most probably obtained is unstable. Theoretically simulated X-ray patterns of structures with randomly packed layers agree well with experimentally observed patterns of diamond-like materials. Since the molecular layers in diamond crystals are packed randomly, a crystal as a whole can attain the 2*H* structure only if it is a nanocrystals. The number of layers in nanocrystals is low, and such crystals may contain only hexagonal layers with a nonzero probability. Hence, the synthesis of macrocrystals with the ideal 2*H* polytype structure is possible theoretically but impossible practically.

Received:

Revised:

Published online:

References

[1] H. O. Pierson, *Handbook of carbon, graphite, diamond, and fullerenes: properties, processing and applications*, Noyes, Park Ridge, NJ, USA **1993**.

[2] J. C. Sung, J. Lin, *Diamond nanotechnology: syntheses and applications*, Pan Stanford, Singapore **2010**.

[3] T. Schuelke, T. A. Grotjohn, *Diam. Relat. Mater.* **2013**, *32*, 17.

[4] Z. Pan, H. Sun, Yi Zhang, C. Chen, *Phys. Rev. Lett.* **2009**, 102, 055503.

[5] C. Frondel, U. B. Marvin, *Nature* **1967**, *214*, 587.

[6] R. E. Hanneman, H. M. Strong, F. P. Bundy, *Science* **1967**, *155*, 995.

[7] F. J. M. Rietmeijer, I. D. R. Mackinnon, *Nature* **1987**, *326*, 162.

[8] P. Nemeth, L. A. J. Garvie, T. Aoki, N. Dubrovinskaia, L. Dubrovinsky, P.R. Buseck, *Nat. Commun.* **2014**, *5*, 5447.

[9] C. G. Salzmann, B. J. Murray, J. J. Shephard, *Diam. Relat. Mater*. **2015**, *59*, 69.

[10] V. A. Greshnyakov, E. A. Belenkov, *J. Exp. Theor. Phys.* **2017**, *124*, 265.

[11] F. P. Bundy, W. A. Bassett, M. S. Weathers, R. J. Hemley, H. K. Mao, A. F. Goncharov, *Carbon* **1996**, *34*, 141.

[12] E. M. Baitinger, E. A. Belenkov, M. M. Brzhezinskaya, V. A. Greshnyakov, *Phys. Solid State* **2012**, *54*, 1715.

[13] E. A. Belenkov, V. A. Greshnyakov, *Phys. Solid State* **2016**, *58*, 2145.

[14] M. T. Yin, *Phys. Rev. B* **1984**, *30*, 1773.

[15] S. Fahy, S. G. Louie, M. L. Cohen, *Phys. Rev. B* **1986**, *34*, 1191.

[16] J. Furthmuller, J. Hafner, G. Kresse, *Phys. Rev. B* **1994**, *50*, 15606.

[17] V. A. Greshnyakov, E. A. Belenkov, *Tech. Phys*. **2016**, *61*, 1462.

[18] E. A. Belenkov, A. E. Kochengin, *Phys. Solid State* **2015**, *57*, 2126.

[19] P. Giannozzi, S. Baroni, N. Bonini, M. Calandra, R. Car, C. Cavazzoni, D. Ceresoli, G.L. Chiarotti, M. Cococcioni, I. Dabo, A.D. Corso, S. de Gironcoli, S. Fabris, G. Fratesi, R.

Gebauer, U. Gerstmann, C. Gougoussis, A. Kokalj, M. Lazzeri, L. Martin-Samos, N. Marzari, F. Mauri, R. Mazzarello, S. Paolini, A. Pasquarello, L. Paulatto, C. Sbraccia1, S. Scandolo, G. Sclauzero, A.P. Seitsonen, A. Smogunov, P. Umari, R.M. Wentzcovitch, *J. Phys.: Condens. Matter*. **2009**, *21*, 395502.

[20] P. Hohenberg, *Phys. Rev.* **1964**, *136* (3B), 864.

[21] J. P. Perdew, A. Zunger, *Phys. Rev. B* **1981**, *23*, 5048.

[22] J. P. Perdew, K. Burke, M. Ernzerhof, *Phys. Rev. Lett*. **1996**, *77*, 3865.

[23] N. Troullier, J. L. Martins, *Phys. Rev. B* **1991**, *43*, 1993.

[24] H. J. Monkhorst, J. D. Pack, *Phys. Rev. B* **1976**, *13*, 5188.

[25] A. Guinier, *Theorie et technique de la radiocristallographie, 3-rd edition*, A. Dunod, Paris **1964**.

[26] D. Kraus, A. Ravasio, M. Gauthier, D. O. Gericke, J. Vorberger, S. Frydrych, J. Helfrich, L. B. Fletcher, G. Schaumann, B. Nagler, B. Barbrel, B. Bachmann, E. J. Gamboa, S. Gode, E. Granados, G. Gregori, H. J. Lee, P. Neumayer, W. Schumaker, T. Doppner, R. W. Falcone, S. H. Glenzer, M. Roth, *Nat. Commun*. **2016**, *7*, 10970.

[27] Y. Nakamuta, S. Toh, *Amer. Miner*. **2013**, *98*, 574.

[28] H. Ohfuji, T. Irifune, K. D. Litasov, T. Yamashita, F. Isobe, V. P. Afanasiev, N. P. Pokhilenko, *Sci. Rep*. **2015**, *5*, 14702.

[29] V. Kvasnytsya, R. Wirth, S. Piazolo, D. E. Jacob, P. Trimby, *J. Superhard Mater*. **2016**, *38*, 71.

[30] F. P. Bundy, J. S. Kasper, *J. Chem. Phys*. **1967**, *46*, 3437.

[31] T. Sekine, M. Akaishi, N. Setaka, K.-I. Kondo, *J. Mater. Sci*. **1987**, *22*, 3615.

[32] S. Welz, M. J. McNallan, Y. Gogotsi, *J. Mater. Process. Technol*. **2006**, *179*, 11.

[33] A. V. Kurdyumov, V. F. Britun, V. V. Yarosh, A. I. Danilenko, V. B. Zelyavskii, J. *Superhard Mater*. **2012**, *34*, 19.

[34] T. B. Shiell, D. G. McCulloch, J. E. Bradby, B. Haberl, R. Boehler, D. R. McKenzie, *Sci. Rep*. **2016**, *6*, 37232.

[35] Z. Cao, W. Zhao, A. Liang, J. Zhang, *Adv. Mater. Interfaces* **2017**, *2017*, 1601224.

[36] P. D. Ownby, Xi Yang, J. Liu, *J Am. Ceram. Soc*. **1992**, *75*, 1876.

[37] Y. Lifshitz, X. F. Duan, N. G. Shang, Q. Li, L. Wan, I. Bello, S. T. Lee, *Nature* **2001**, *412*, 404.

[38] E. A. Belenkov, M. M. Brzhezinskaya, V. A. Greshnyakov, *Diam. Relat. Mater*. **2014**, *50*, 9.

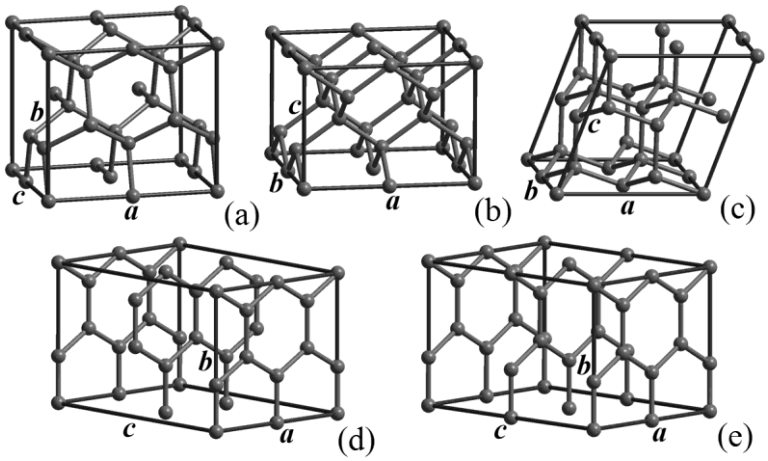

Figure 1. Geometrically optimized unit cells of hexagonal diamond (a), cubic diamond (b and c), and AB and AA graphites (d and e, respectively).

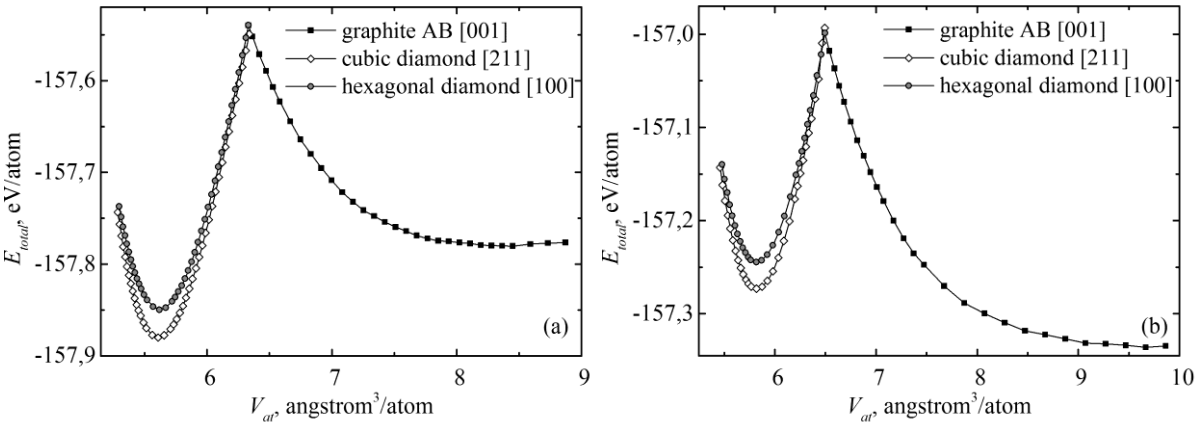

Figure 2. Plots of total energy (E_{total}) versus atomic volume (V_{at}) for the «graphite AB → diamond-like phases» calculated by the DFT-LDA (a) атd DFT-GGA (b) methods.

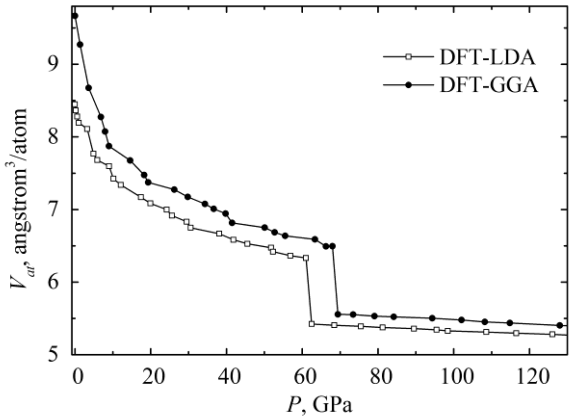

Figure 3. Atomic volume (V_{at}) versus pressure (P) for the «graphite AB → hexagonal diamond» phase transition. The plot has been constructed based on calculations by the DFT-LDA and DFT-GGA methods.

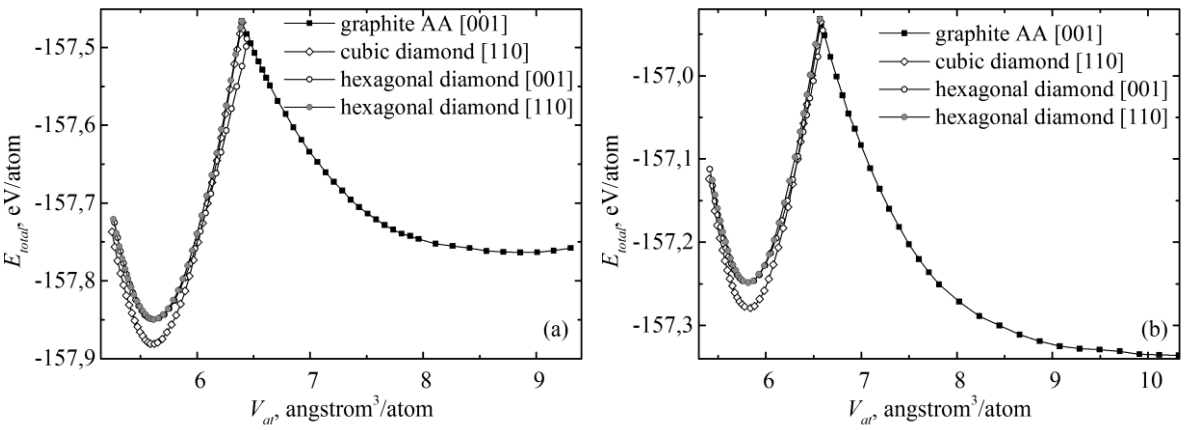

Figure 4. Plots of total energy (E_{total}) versus atomic volume (V_{at}) for the «graphite AA → diamond-like phases» calculated by the DFT-LDA (a) and DFT-GGA (b) methods.

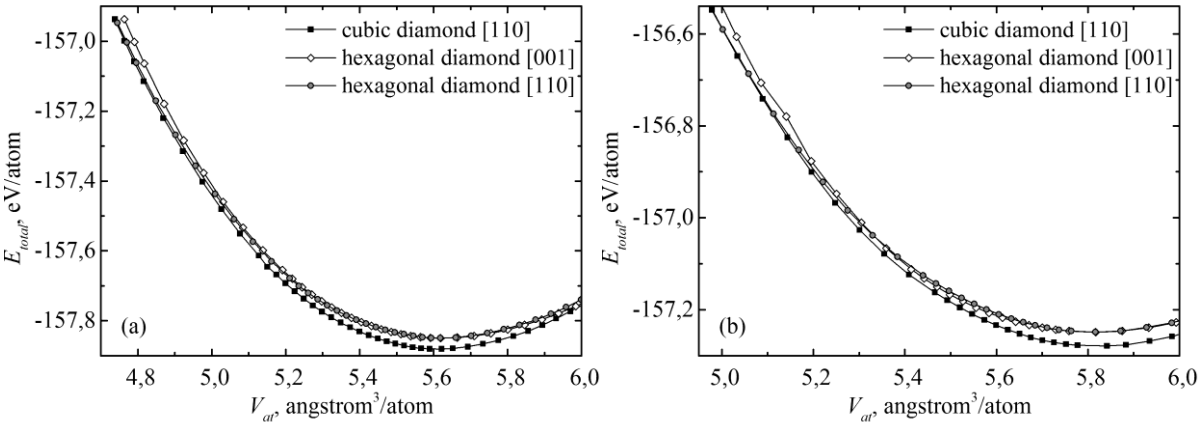

Figure 5. Dependences of E_{total} versus V_{at} for the «3*C* diamond [110] → 2*H* diamond» calculated by the DFT-LDA (a) and DFT-GGA (b) methods.

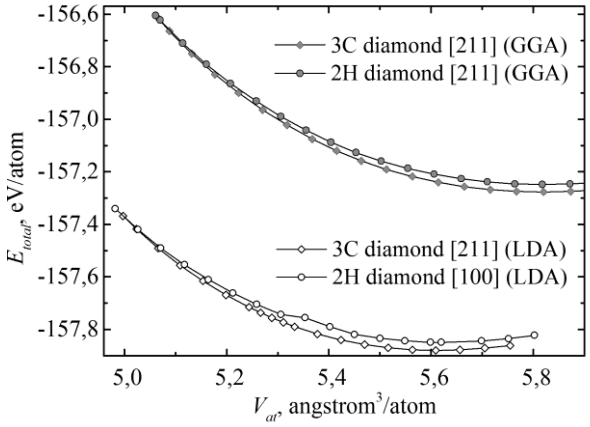

Figure 6. Dependences of E_{total} versus V_{at} for the «3*C* diamond [211] → 2*H* diamond [100]» calculated by the DFT-LDA and DFT-GGA methods.

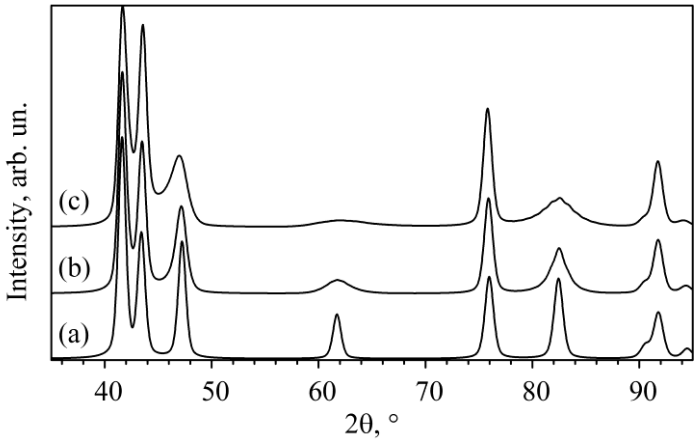

Figure 7. Powder X-ray patterns of the hexagonal diamond (a) and mixtures of diamond polytypes with the average hexagonality of 88% (b) and 74 % (c) ($\lambda_{Cu\text{-}K\alpha}$ = 1.5405 Å, mean crystal size is 150 Å).

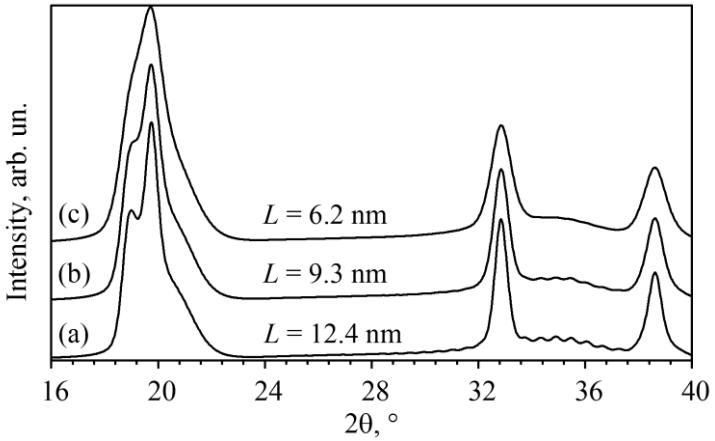

Figure 8. Powder X-ray patterns of mixtures of diamond polytypes with the average hexagonality of 50% (b) and crystallite sizes (*L*) of 124 (a), 93 (b) and 62 Å (c) ($\lambda_{Mo\text{-}K\alpha}$ = 0.71073 Å).

Table 1. Unit cell parameters (*a*, *b*, *c*, β), equilibrium volumes (V_0) and total energies (E_{total}) of carbon compounds (the values calculated by the DFT-LDA method are presented without brackets, while those calculated by the DFT-GGA method are given in brackets). Bravais lattices: T – simple tetragonal; O – simple orthorhombic; M – simple monoclinic.

Phase	2*H* diamond	3*C* diamond		AB graphite	AA graphite
Bravais lattice	O	T	M	O	O
a [Å]	4.155 (4.203)	5.029 (5.095)	4.352 (4.405)	4.265 (4.308)	4.927 (4.975)
b [Å]	4.329 (4.377)	5.029 (5.095)	5.026 (5.091)	4.931 (4.977)	4.265 (4.308)
c [Å]	4.998 (5.060)	3.556 (3.600)	4.352 (4.405)	6.428 (7.361)	6.745 (7.708)
β [°]	90.00	90.00	70.52	90.00	90.00
V_0 [Å^3/atom]	5.619 (5.817)	5.622 (5.874)	5.608 (5.820)	8.450 (9.864)	8.859 (10.325)
E_{total} [eV/atom]	-157.85 (-157.25)	157.88 (-157.28)	-157.88 (-157.28)	-157.78 (-157.34)	-157.76 (-157.34)

Table 2. Characteristics of direct phase transitions of carbon precursors to the cubic and hexagonal diamonds ($[hkl]_i$-strain directions of the precursors (i = 1) and final diamond-like phases (i = 2), and also atomic volumes (V_{trans}), energy barriers (ΔE_{trans}) and pressures (P_{trans}) of phase transitions; the values calculated by the DFT-LDA method are presented without brackets, while those calculated by the DFT-GGA method are given in brackets).

Precur-sor	$[hkl]_1$	Phase	$[hkl]_2$	V_{trans}, Å^3/atom	ΔE_{trans}, eV/atom	P_{trans}, GPa
AB graphite	001	2*H* diamond	100	6.332 (6.495)	0.241 (0.337)	61.0 (68.0)
		3*C* diamond	211	6.346 (6.489)	0.235 (0.340)	60.2 (68.4)
AA graphite	001	2*H* diamond	001	6.453 (6.599)	0.275 (0.391)	57.4 (65.8)
			110	6.396 (6.567)	0.297 (0.404)	61.1 (67.2)
		3*C* diamond	110	6.400 (6.574)	0.296 (0.401)	60.8 (66.9)
3*C* diamond	110		110	4.745 (4.983)	0.926 (0.731)	380 (300)
		2*H* diamond	001	<4.745 (<4.983)	>0.926 (>0.901)	>380 (>300)
	211		100	4.997 (5.065)	0.511 (0.664)	303 (354)